# Status of the $T_{20}$ Experiment at VEPP–3

**S.G.Popov, S.I.Mishnev, D.M.Nikolenko, D.V.Petrov, I.A.Rachek, A.V.Sukhanov, D.K.Toporkov, E.P.Tsentalovich[1], A.V.Volosov, and B.B.Wojtsekhowski[2]**

*BINP, Novosibirsk, Russia*

**C.E.Jones, R.S.Kowalczyk, M.Poelker, D.H.Potterveld and L.Young**

*Argonne National Laboratory, Argonne, IL, USA*

**R.J.Holt**

*University ol Illinois, Urbana-Champaign, IL, USA*

**R.Gilman**

*Rutgers University, Piscataway, NJ, USA*

**E.R.Kinney**

*Colorado University, Boulder, CO, USA*

**K.P.Coulter**

*University of Michigan, Ann Arbor, MI, USA*

**J.A.P.Theunissen, C.W.de Jager, H.de Vries,**

*NIKHEF-K, Amsterdam, The Netherlands*

**V.V.Nelyubin, V.V.Vikhrov**

*INP, St.-Petersburg, Russia*

**A.N. Osipov, V.N. Stibunov**

*INR, Tomsk, Russia*

# 1 Introduction

It is difficult to overestimate the importance of a comprehensive analysis of the simplest nuclear system - a deuteron. Electromagnetic probes are appropriate for an experimental study of the deuteron, due to the transparent interpretation of the results. Polarization experiments are of special interest since the polarization observables, such as $T_{20}$ in elastic $e-d$ scattering, are sensitive to very delicate aspects of nucleon-nucleon interactions, such as isoscalar meson-exchange currents, relativistic effects and quark degrees of freedom.

## 1.1 $T_{20}$ experiments: finished, running and proposed

In the last decade a few experiments were performed with polarization techniques in electron–deuteron elastic scattering [1-6]. Different approaches were used: polarimeters of recoil deuterons at BATES [1, 2], a cryogenic $^{15}N\vec{D}_3$ target at Bonn [3] and an internal gaseous polarized target (first a jet target and

[1]Present address: MIT Bates, MA, USA

[2]Present address: CEBAF, Newport News, VA, USA

later a storage cell) at VEPP-3, Novosibirsk [4, 5, 6]. Experiments at VEPP-3 were carried out by an Argonne / Novosibirsk / St. Petersburg / Tomsk / NIKHEF collaboration. Note that as far as we know the experiments at Bates and at Bonn are finished and there are no plans to continue these experiments in order to improve the accuracy or to move to a different momentum transfer range.

A program of intensive study of spin properties of the deuteron is planned for CEBAF. The proposed experiment 93-04 is a continuation of the Bates experiment up to a momentum transfer 6.8 $fm^{-1}$ with a new polarimeter "POLDER" [7]. Two other experiments will use the $\vec{D}(\vec{e}, e'd)$ reaction with a cryogenic vector polarized $N\vec{D}_3$ target. The first experiment (spokesperson J.Mitchell) will use a magnetic spectrometer in Hall C. The second experiment (spokespersons B.Wojtsekhowski and D.Crabb) will measure the monopole deuteron form factor using the CLAS spectrometer in Hall B. Also there is discussion about doing a $T_{20}$ experiment at HERA during the HERMES experiment. Note that the experiments at CEBAF are not approved so far [3] and the results of the measurements are expected to be obtained not earlier than 1998. In addition, these experiments are based on a different approach with different systematic uncertainties than the internal target experiment at VEPP-3 and therefore do not reduce the importance of the experiment proposed in this paper.

Fig.1 shows the world $T_{20}$ data acquired to date.

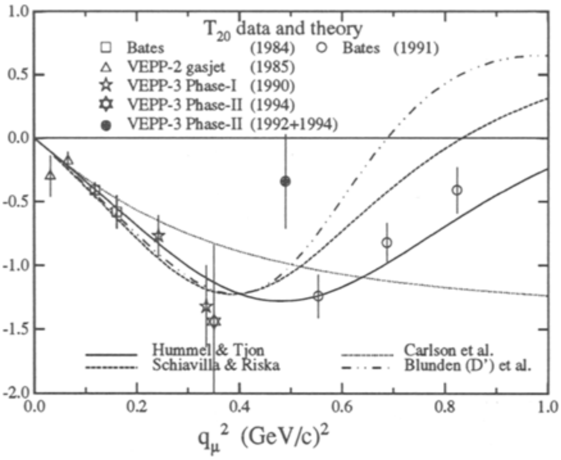


Figure 1: World $T_{20}$ data

[3] The "POLDER" experiment is now approved and given a high priority

### 1.2 Three phases of the $T_{20}$ experiment at VEPP-3

Started in 1987, the experiment at VEPP-3 was planned to be conducted in three phases:

I. the use of a simple passive storage cell and a conventional atomic beam source;
II. an active high-density storage cell with a conventional source;
III. a laser-driven source and a high density passive storage cell.

At the final phase of this experiment it was expected to be able to make measurements of $T_{20}$ up to a momentum transfer range 4.5 $fm^{-1}$.

## 2 Phase-I and Phase-II experience

### 2.1 Phase-I

The storage cell of Phase–I of the experiment was installed in the VEPP-3 straight section in February 1988. The detector set-up , the ABS and the holding field magnet were the same as for the polarized jet experiment. That is why while the total increase of the target thickness as compared with the plain jet target was a factor of about 15, the achieved gain was only 3. The main objectives of Phase-I were to show the feasibility of the storage cell concept, to investigate depolarization processes and to collect data on $T_{20}$ in elastic scattering for 1...2.5 $fm^{-1}$. The latter was successfully done in a period from August 1988 to April 1989. The analysis of the elastic scattering data at the lowest momentum-transfer value allowed us to extract the properties of the storage cell internal target by normalizing to theoretical predictions: the target thickness in central part of the cell viewed by the detectors, $t_{vis} = 3 \cdot 10^{11} atoms/cm^2$; average degree of tensor polarization $P_{zz} = 0.57 \pm 0.05$. Figure 2 presents the measurements of the asymmetry at this lowest-Q value during the experiment. No substantial degradation of the polarization could be seen over a 7-months period. This demonstrated that the drifilm coating was of sufficient radiation hardness.

### 2.2 Phase-II

The first example of a movable storage cell was installed on the VEPP-3 straight section in May, 1989. That was a 'clam-shell' design driven by a single motor via a rotating vacuum feedthrough. First successful closing of the cell with the beam of 2 GeV electrons in VEPP-3 was achieved on July 27, 1989. The same ABS was used. A new detector was constructed and installed in February, 1991. In 1990 a long-term data-taking run has been carried out

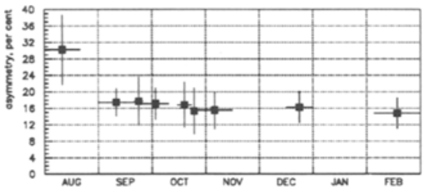


Figure 2: Asymmetry at low-Q measured during Phase–I.

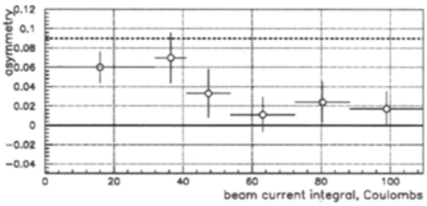


Figure 3: Low-Q polarimeter asymmetry measurements during the winter-94 run. Dashed line - the predicted value for $P_{zz} = 1.0$.

to measure the averaged tensor polarization of the target with the active cell. The run showed that the polarization degree is close to zero.

In principle, the reason of low measured target polarization might be one or several of the following:

- low polarization of atoms coming from the ABS due to inefficient RF transitions;
- high level of deuterium molecules from the ABS as well as of unpolarized residual gas inside the cell;
- depolarization by the intense pulsed magnetic field of the electron beam;
- systematic errors related to non-equal luminosity integrals collected in different polarization states;
- systematic errors related to high (and unknown) level of background processes (mainly from deuteron electrodisintegration) in the data which were selected as elastic events;
- bad cell coating;

Some of these effects are known to be negligible, others can be accurately estimated and corrected for:

- During this run and all further Phase-II runs the efficiency of the RF transitions was permanently monitored by a Rabi polarimeter and was observed to be close to 100%.
- Contribution of deuterium molecules $\approx 4\%$ was obtained from the measured dissociation fraction and the known geometry of the atomic beam source;
- Contribution of the residual gas inside the cell $\approx 7\%$ was estimated from the measured vacuum in the experimental straight section;
- Depolarization by the electron beam has been studied experimentally and theoretically in Phase-I [8] and that experience was used in design of the Phase-II. This allowed us to be sure that such a depolarization is negligible.

- Polarization states (the sign of $P_{zz}$) were changed every 1-2 minutes, time and collected beam charge in each state were measured. It was found that integrals of beam current in each polarization state differed by less than 1% for a long-term run. Moreover, this difference is taken into account.
- Our confidence in the data analysis is based on our experience with the similar detector systems in Phase-I and in earlier experiments. Detailed discussions on the requirements for a detection system and an analysis procedure can be found in ref. [9].

The behaviour of the drifilm cell coating under real experimental conditions is the least known item. A number of reasons might cause a degradation of the cell coating:

- irradiation by synchrotron light. Its influence on drifilm properties is still not known in detail. It is obvious that this effect can be suppressed by installation of screens and light absorbers in the proper places. Unfortunately, it was found that screens placed just in front of the cell are not sufficient since there remains light coming from a rather big angle which cannot be screened. That is apparently light from the bending magnet reflected on an inner surface of the VEPP-3 vacuum chamber.

- radiation damage caused by electrons from the electron beam. Again no quantitative data on this effect is available.

- direct hitting of the cell by the electron beam. That is unlikely when the cell is stable but might occur when a movable cell is closing and the electron beam was not aligned properly.

- mechanical damage. This could occur either because of surface defects during initial drifilm covering which lead to slicing off part of the coating during installation of the cell, or due to a malfunction of the cell-moving mechanism causing an excessive strain. The latter is potentially dangerous only for a movable cell.

In the latter two cases one would expect an instantaneous degradation of the coating and, hence, of the target polarization. In the former two the degradation should be gradual. So the most probable reason of the low measured asymmetry is damage of the drifilm cell coating.

The cell has been removed from the VEPP-3 vacuum chamber in August 1990 during the summer shutdown of the ring. Damages of the drifilm coating have been observed in several places as well as dark spots on the inner surface of the cell related to an irradiation by synchrotron light.

Data were accumulated at an electron energy of 2 GeV in a period December 1991 to May 1992. The integrated charge was 156 kC. As in Phase-I we have binned the data in two q-ranges and the datum at the lowest value of Q was used to determine the average $P_{zz}$ and the thickness of the target. We thus found that $P_{zz} = 0.68 \pm 0.22$ and the target thickness $t_{vis} = (3.0 \pm 0.5) \cdot 10^{12} atoms/cm^2$

However, during this run a serious problem was encountered – a high background rate spoiled the energy and spatial resolution of the particle detectors and enlarged the dead-time of the read-out electronics. That is why we had to work with a substantially (factor 2.5) smaller electron beam current than the VEPP-3 storage ring can potentially provide. The origin of the background was investigated and associated with electrons from the beam "halo" hitting the cell wall. To alleviate this problem, four movable collimators were installed during the summer–1992 shutdown of the ring. Further measurements have shown that the collimators did decrease the background rate by a factor 3–10 for various detectors. Besides, a new read–out electronics, based on INMOS transputers was introduced, which reduced the dead–time by an order of magnitude.

One more data-taking run at 2 GeV electron energy was performed from November 1992 to April 1993. The asymmetry at the lowest Q-value ($3 \pm 0.25$ $fm^{-1}$) was found to be $a = -0.07 \pm 0.16$, while the expected value is $+0.73$ for $|P_{zz}|$=1.0, suggesting a degradation of the drifilm coating. Note that by the end of this run the total amount of beam charge passed through the cell since it was installed in 1991 was about 500 kC.

This result has shown once again that it is essential to have a fast monitor of the average tensor polarization in the target. It was decided to install an additional detector arm to detect electrons scattered over a small angle ($\approx 7°$), to be able to take data of elastic scattering at low Q (around 1 $fm^{-1}$) where the cross-section is high and the asymmetry is known with high accuracy. Such a detector was installed in May 1993.

A short special run with the same storage cell was carried out in June July 1993 to test the new detector and to measure the polarization of the target. In this run the holding field direction ($\theta_H = 83°$) was chosen such as to provide a maximal asymmetry for the low-Q polarimeter kinematics. An integrated beam charge of 7.3 kC was collected. It was clearly shown that such a simple "low-Q" polarimeter is an effective tool for checking the polarization i.e. a state of the cell coating. The asymmetry was measured to be $a = 0.093 \pm 0.030$ which corresponds to the target polarization of $P_{zz} = 0.69 \pm 0.22$. On the other hand, this result with the low-Q polarimeter clearly contradicts the value obtained from the normalization of the actual $T_{20}$–data at the low Q bin.

Despite of the positive result with the low-Q polarimeter run, it was decided to take out the storage cell during the summer–1993 shutdown of the VEPP-3 to cover the cell surface with "fresh" drifilm.

The last data-taking run has started in October 1993. However, due to various instrumentation problems only in February 1994 did we start running with the polarized target. Figure 3 shows the asymmetry measured by the low-Q polarimeter during the run. One can see that somewhere in the middle of the run the polarization decreased, implying that something disastrous happened with the cell coating. However, one has to take into account that by that time (March 1994) the integrated charge passed through the closed cell since it was installed in August 1993 was about 150 kC.

Before and after this run there were also short runs with unpolarized hydrogen and deuterium targets as well as with an 'empty' cell to calibrate the detector and to check the analysis. Such runs have been regularly performed during previous data taking runs also. These runs clearly showed that there is no false asymmetry from either the main detector or the low-Q polarimeter. The obtained energy and spatial resolution of the detector are listed in the Table 1 together with the design values. One can see that the detector parameters are slightly worse than expected. Nevertheless they are sufficient to select the events of elastic scattering at a momentum transfer up to at least 4.0 $fm^{-1}$. However, we are going to improve the detector performance mostly by upgrading the tracking system. This includes the installation of the new vertex chambers with an improved design and the replacing a part of $\theta$–wire-planes in electron arms by the ones with twice smaller wire spacing.

| Parameter | designed | measured |
|---|---|---|
| angle resolution FWHM, degrees | 0.6 | 1.8 |
| vertex position resolution, FWHM : | | |
| across the beam, mm | 1.0 | 2.5 |
| electron energy resolution, % | 7.0 | 8.5 |
| hadron energy resolution, FWHM, MeV | 15 | 14 |

Table 1: Detector Parameters, designed and measured

## 2.3 Data analysis

The layout of the particle detector is shown in Fig. 4. This detector is based on the same principle as our previous detectors [9] for internal target experiments: large angular-acceptance non-magnetic instruments detecting the scattered electron and the knocked-out hadron in coincidence. The present detector package includes a set of wire chambers for tracking, a hodoscope of plastic scintillators for a hadron detection and a layered CsI(Tl)/NaI(Tl) electron calorimeter.

The crucial task for the data analysis is the separation of elastically scattered deuterons from the much greater flux of protons from inelastic and quasi-elastic scattering. This separation uses constraints on the vertex position, on

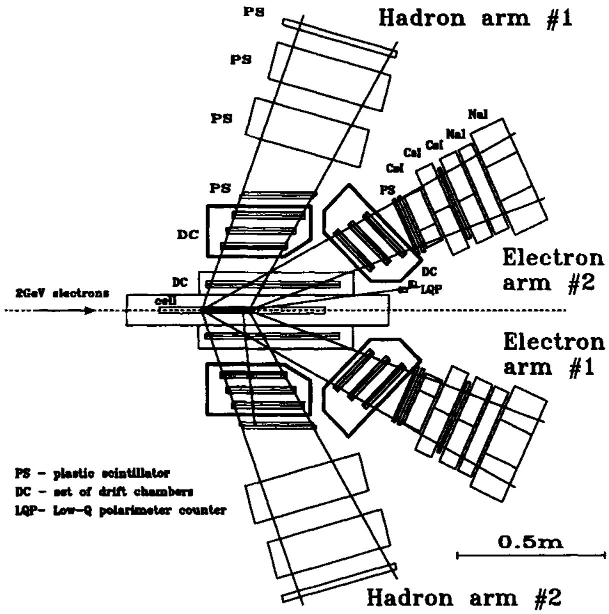


Figure 4: Layout of the detector set-up.

the electron energy deposited in the calorimeter, the kinematical correlation between the electron and deuteron scattering angles and energies and the differences in $dE/dx$ in the scintillation counters.

The data analysis sequence comprises a number of stages:

1. Immediate rejection of events obviously not relevant to elastic scattering. The following cuts are used at this stage:

   - an energy deposition in the calorimeter exceeding $\approx$1.5 GeV;
   - the particle stopping in the 3rd plastic scintillator of the deuteron arm. This constrains the deuteron energy to a range from 80 to 150 MeV, corresponding to a momentum transfer range in elastic scattering of 0.55 to 0.75 GeV/c;

2. Conversion of the raw TDC and ADC data to physical parameters : angles and energies of detected particles, coordinate of escape point. Data from calibration frequently performed during the data run are used and various corrections are carried out at this stage.

3. Derivation of the correlation and identification parameters.

4. Final data analysis on a graphics workstation using PAW software package [10].

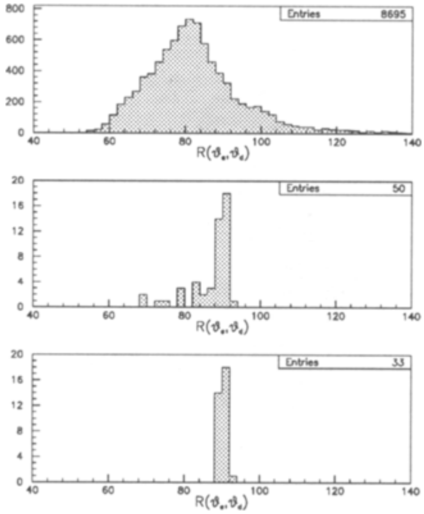


Figure 5: Histograms of the $R(\theta_e, \theta_d) = \theta_e + \theta_d$ correlation parameter. The upper histogram shows all events, the middle one the events left after applying all cuts except $R(\theta_e, \theta_d)$ and the lower one the events surviving all cuts.

The following six cuts were applied to single out the elastic scattering events when analyzing data of the winter-1994 run:

| | |
|---|---|
| • Energy of scattered electron | >1500 MeV |
| • Vertex position transverse to the electron beam direction [mm] | -4...4 |
| • Correlation between electron and deuteron azimuthal angles, $R(\phi_e, \phi_d) = \phi_e - \phi_d - \pi$ | $-2.5° \ldots 2.5°$ |
| • Correlation between electron and deuteron polar angles, $R(\theta_e, \theta_d) = \theta_e + \theta_d$ | $88° \ldots 93°$ |
| • Correlation between deuteron energy and electron scattering angle, $R(E_d, \theta_e) = 10 \cdot \theta_e - A_3/12$ [a.u.] | 135...175 |
| • $\Delta E - E$ hadron identification parameter $I(\Delta E, E) = (A_3 + 300) \cdot (A_1 + A_2 - 200)/1000$ [a.u.] | 170...300 |

Fig. 5 shows histograms of $R(\theta_e, \theta_d)$ correlation parameter before and after background rejection.

The preliminary analysis of the winter-1994 run gave the following results : the time-averaged target polarization obtained from the low-$Q$ polarimeter data $P_{zz} = 0.52 \pm 0.08$; $T_{20}$ values for two ranges of momentum transfer were found to be $-1.44 \pm 0.6$ for $q^2 = 0.35(Gev/c)^2$ and $-0.36 \pm 0.75$ for $q^2 = 0.50(Gev/c)^2$. Combining the high-$Q$ bin value with that obtained in the earlier measurement we finally get $T_{20} = -0.34 \pm 0.37$. The results are shown in fig. 1.

### 2.4 Summary of Phase-I and Phase-II experience

Summing up the results and experience of Phase–I and Phase–II of the Novosibirsk $T_{20}$ experiment we would like to stress the following.

- The storage cell concept to increase the thickness of polarized internal target proved to be feasible both for 'passive' and for 'active' cell design. However, a movable cell is more susceptible to potential damaging of the drifilm coating. This reason together with some others mentioned in next section made us choose a stable cell for the next phase of the experiment.
- The lifetime of the drifilm coating exceeds at least half a year of exposure at the interaction point of the storage ring in which **more than ≈150 kC** of integrated beam charge can be collected.
- The particle detectors and data acquisition system have shown an adequate performance. However a number of minor upgrades (mainly in the tracking system) will be carried out.
- Collimators installed in a proper place of the ring are effective in suppressing the high background rate produced by stray particles hitting the cell walls.
- It is very important to have a fast monitor of the average target polarization to be able to check the state of the drifilm coating during the run and to obtain an accurate value of degree of target polarization. It was shown that the Low-Q elastic scattering polarimeter should prove to be an effective tool to meet these needs.
- It is very useful to be able to change the cell quickly when the degradation of the polarization is detected. Such a design of the cell is being considered now for the next phase of the experiment.

We believe that we can now perform a successful run in the current phase, but a meaningful statistical result in a momentum transfer range $q > 3.5 fm^{-1}$ would require a long period of data-taking (about 2 years), which would interfere with the development of the Phase–III. Furthermore, in the present phase we can not replace the cell quickly, but have to wait until the shutdown of the VEPP-3 ring (usually in summer). That would further increase the time necessary to collect the required amount of data. As will be shown below, the successful development of Phase–III would provide better statistics in the same period, providing precision measurements most quickly.

# 3 Phase–III

A substantial increase in the luminosity will be achieved by the use of a novel source of polarized atoms which is based on the spin-exchange optical pumping technique and has been developed at Argonne National Laboratory [11].

Molecular deuterium is dissociated in an RF discharge and travels into a drifilm coated spin-exchange cell containing potassium vapor. The potassium is optically pumped and polarized by a laser beam with circular polarization in the presence of a high magnetic field. Electron polarization of potassium is transferred to deuterium atoms through spin-exchange collisions. The mixture of atoms passes through a transport tube where the potassium atoms are absorbed in a teflon sleeve. The deuterium atoms enter the storage cell after passing through an RF transition unit. The efficiency of a similar transition unit at low magnetic field and in the 20 MHz frequency region were measured to be $\varepsilon = 0.92 \pm 0.05$ [12]. The efficiency for the transitions 3→5 and 2→6 for deuterium still has to be tested. A high electron polarization of the atoms from the source (about 80%) has been measured at flow rates of $2{\cdot}10^{17}$ at/sec, while lower values were measured for flow rates exceeding $1{\cdot}10^{18}$ at/sec. The cell is a passive one with a 23×12 mm elliptical cross section and a 400 mm length manufactured from 0.1 mm thick aluminum. The cell is drifilm coated and should provide a total target thickness of about $1{\cdot}10^{14}$ at/cm$^2$ at a flow rate of $1{\times}10^{17}$ at/sec. For these estimations a cylindrical tube with a 16 mm diameter and a 400 mm length at a 150°C wall temperature was assumed.

The presence of a potassium vapor in the flow forces us to keep most parts of the target (including the storage cell) under high temperature to prevent potassium condensation. It is obvious that a movable ( like phase-II cell ) and heated cell would be complicated to design. Moreover, a fixed cell can be made with a small wall thickness, thus significantly lowering the background. For these reasons we chose a fixed storage cell.

An important feature of Phase–III is compressing the electron beam near the experimental straight section through changes in the VEPP-3 electron beam optics (Fig. 6). We plan to add two new quadrupoles ( DD and FD ) inside the experimental straight section and to change the gradient of several existing quadrupoles ( see Table 2 ).

| Lens | D1 | F1 | D2 | F2 | DD | FD | D3 | F3 | D4 | F4 |
|---|---|---|---|---|---|---|---|---|---|---|
| Phase I,II | -1.67 | 1.67 | -1.67 | 1.67 | – | – | -1.67 | 1.67 | -1.67 | 1.67 |
| Phase III | -1.48 | 1.48 | -1.67 | 2.15 | -2.88 | 4.30 | -2.15 | 1.67 | -1.67 | 1.48 |

Table 2: Quadrupole gradients ( kG/cm ).

The compressed electron beam provides new possibilities:

- to use a stable storage cell with a small cross section.
- to apply an effective differential pumping scheme ( two steps with high speed pumps and a tube with a conductance limiter between them) allowing acceptable vacuum conditions in the VEPP-3 ring at the high flux of atoms from an LDS (Fig. 7).

- size of DD and FD quadrupoles may be made small, which is important due to the restricted space at the straight section.

| Phase | I | II | III |
|---|---|---|---|
| Polarized deuterium<br>source type<br>Flux [$atoms/sec$]<br>$P_{zz}$ | <br>ABS<br>$4 \cdot 10^{15}$<br>$\approx 1$ | <br>ABS<br>$4 \cdot 10^{15}$<br>$\approx 1$ | <br>LDS<br>$3 \cdot 10^{17}$<br>$P_e \cdot K_{rf} \cdot K_{ds} =$<br>$.8 \cdot .9 \cdot .6 = .43$ |
| Cell type<br>Cell size [$mm^3$] | fixed<br>$24 \times 46 \times 940$ | movable<br>$9(13) \times 17(21.5) \times 569$ | fixed<br>$13 \times 24 \times 400$ |
| $t$ – Visible target<br>thickness [$atoms/cm^2$]<br>Target $P_{zz}$ | <br>$3 \cdot 10^{11}$<br>0.6 | <br>$3 \cdot 10^{12}$<br>0.6 | <br>$2 \cdot 10^{14}$<br>0.8· 0.43=0.35 |
| Figure of merit<br>$t \cdot P_{zz}^2$ | <br>$10^{11}$ | <br>$10^{12}$ | <br>$2.5 \cdot 10^{13}$ |
| *Detector system*<br>$e^-$ scattering angle<br>$e^-$ $\Delta\phi \times N_{syst}$<br>*registration :*<br>tracking<br>hadron energy<br>electron energy | <br>$10^\circ - 20^\circ$<br>$40^\circ \times 4$<br><br>yes<br>yes<br>no | <br>$20^\circ - 30^\circ$<br>$60^\circ \times 2$<br><br>yes<br>yes<br>yes | S A M E |
| Anti-background<br>scrapers | <br>no | <br>yes | <br>yes |
| VEPP-3 optics<br>beam size $\sigma_z/\sigma_x$ [$mm$] | old<br>0.35/1.4 | old<br>0.35/1.4 | new<br>0.20/0.7 |

Table 3: Parameters of the three phases of the $T_{20}$ experiment at VEPP-3. $P_e$ – atomic electron polarization, $K_{rf}$ – efficiency of radio-frequency transition unit, $K_{dc}$ – dissociation fraction.

The electron beam lifetime in Phase–III will be 2-3 times less than in Phase–II because of the increase in target thickness. Since it is the electrons scattered on the storage cell walls that define the singles rate of the detectors, one might expect an increase of the background. On the other hand, the smaller wall thickness of the new storage cell and the smaller size of the electron beam in the cell should reduce the background even more significantly. Therefore we expect background conditions in Phase–III to be better than in Phase–II.

The main experimental parameters of all phases are shown in Table 3.

An experimental result for the $T_{20}$ which one can get in Phase–III is shown in Fig. 8. For this calculation the Paris potential was used, the target and

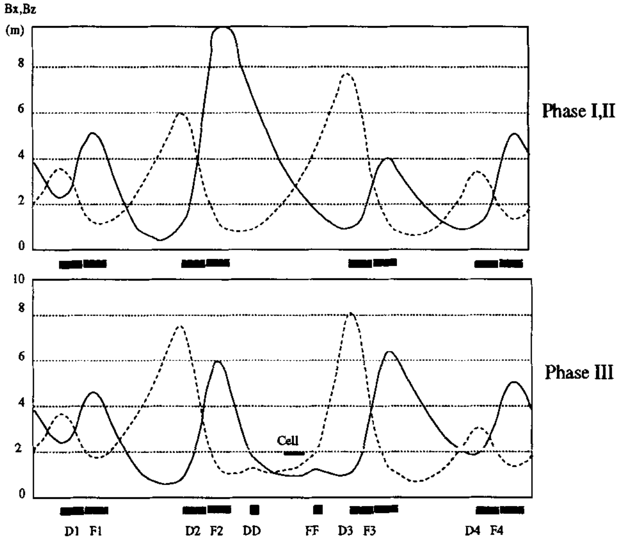


Figure 6: Radial (solid line) and vertical (dashed line) beta-functions in the experimental straight section of VEPP-3, before (upper panel) and after (lower panel) upgrade of the ring optics.

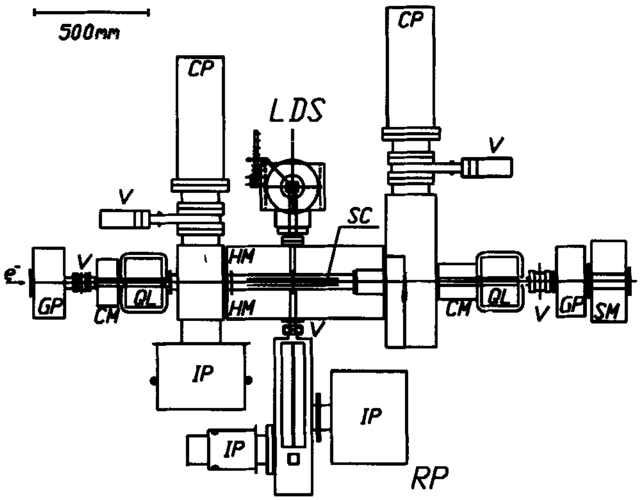


LDS-Laser-Driven Source, SC-storage cell, RP-Rabi polarimeter, HM-holding field magnet, QL-quadrupole Lense,CM-compensated magnet, SM-sextupole magnet, GP-getter pump, CP-cryopump IP-ion pump., V-valve

Figure 7: Top view of the Phase–III experimental straight section

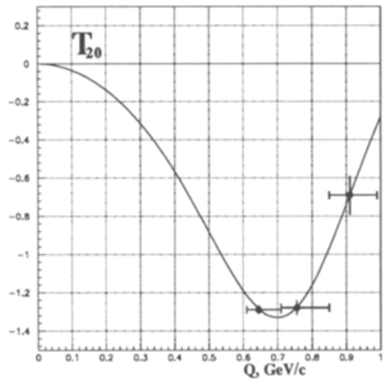


Figure 8: The expected accuracy of the $T_{20}$ measurement in Phase–III. Calculations were performed using the Paris potential for an integrated charge of 400 kC. Target and detector parameters were taken from Table 3.

detection system parameters were taken from Table 3, an integrated electron beam charge was assumed to be 400 kC (or 100 days of beam time). The momentum transfer ranges for the three points are 3.1 - 3.6, 3.6 - 4.3 and 4.3 - 5.0 $fm^{-1}$. One can see that the proposed measurement will cover approximately the same momentum transfer range as in [2] but with higher accuracy.

# 4 Conclusion

Summing up the above we would like to note that

- experiments in Phase–I and Phase–II gave new results, besides operational experience with a storage-cell polarized target in an electron storage ring. This experience was used in the design of Phase–III of the experiment and allows us to be confident in its success;

- the new intense laser-driven source of polarized deuterium atoms, the new VEPP-3 electron beam optics and the new design of the straight section should result in a figure of merit in Phase–III about a factor of 30 larger than that in Phase–II;

- a precise measurement of $T_{20}$ in an interesting region of momentum transfer will be performed within one or two years.

*This research was supported in part by the U.S. Department of Energy, Nuclear Physics Division, under contract W-31-109-ENG-38; by the Russian Fund for Fundamental Research, under contract 123.06; by the Netherlands' Organization for Scientific Research (NWO), under contract nr. 713-119 and by the International Science Foundation, Grant N RBC000-PH1-6689-0925.*

# References


[1] M.E.Schultze *et al.*, Phys. Rev. Lett. **52**(1984)597.

[2] I.The *et al.*, Phys. Rev. Lett. **67**(1991)173.

[3] B.Boden *et al.*, Z.Phys. **C49**(1991)175.

[4] V.F.Dmitriev *et al.*, Phys. Lett. **157B**(1985)143.

[5] R.Gilman *et al.*, Phys. Rev. Lett. **65**(1990)1733.

[6] E.P.Tsentalovich *et al.*, Proc. of PAN XIII International Conf., Perugia, June 28 - July 2, 1993, p. 797, Ed. by A.Pascolini.

[7] S.Kox *et al.*, Nucl. Instr. and Meth. **A346**(1994)527.

[8] R.Gilman *et al.*, Nucl. Instr. and Meth. **A327**(1993)277.
K.P.Coulter, An active storage cell for a polarized gas internal target, submitted to Nucl. Instr. and Meth.

[9] L.G.Isaeva *et al.*, Nucl. Instr. and Meth. **A325**(1993)16.
J.A.P.Theunissen *et al.*, Nucl. Instr. and Meth. **A348**(1994)61.
E.P.Tsentalovich. Doctor Thesis (unpublished), Budker INP, Novosibirsk, 1991.
J.A.P.Theunissen. Doctor Thesis (unpublished), NIKHEF, Amsterdam, 1995.

[10] R.Brun *et al.* PAW - Physics Analysis Workstation. The complete Reference. CERN, Geneva, 1989.

[11] K.P.Coulter *et al.*, Phys. Rev. Lett. **68**(1992)174.

[12] A.Zghiche *et al.*, Proc. of Workshop on Polarized Gas Targets for Storage Ring, Heidelberg, 23-26 Sept. 1991, p.103, Ed. by H.G.Gaul, E.Steffens and K.Zapfe.